Fluorescence lifetime fluctuations of single molecules probe local density fluctuations in disordered media: A bulk approach

R. A. L. Vallée[a)]
Applied Optics Group, MESA+ Institute for Nanotechnology, University of Twente, P.O. Box 217, 7500 AE Enschede, The Netherlands and Laboratory for Spectroscopy and Photochemistry, Department of Chemistry, Catholic University of Leuven, B-3001 Heverlee, Belgium

N. Tomczak and G. J. Vancso
Materials Science and Technology of Polymers, MESA+ Institute for Nanotechnology, University of Twente, P.O. Box 217, 7500 AE Enschede, The Netherlands

L. Kuipers and N. F. van Hulst[b)]
Applied Optics Group, MESA+ Institute for Nanotechnology, University of Twente, P.O. Box 217, 7500 AE Enschede, The Netherlands

(Received 23 September 2004; accepted 3 January 2005; published online 17 March 2005)

We investigated the nanometer scale mobility of polymers in the glassy state by monitoring the dynamics of embedded single fluorophores. Recently we reported on fluorescence lifetime fluctuations which reflect the segmental rearrangement dynamics of the polymer in the surroundings of the single molecule probe. Here we focus on the nature of these fluorescence lifetime fluctuations. First the potential role of quenching and molecular conformational changes is discussed. Next we concentrate on the influence of the radiative density of states on the spontaneous emission of individual dye molecules embedded in a polymer. To this end we present a theory connecting the effective-medium theory to a cell-hole model, originating from the Simha–Somcynsky free-volume theory. The relation between the derived distributions of free volume and fluorescence lifetime allows one to determine the number of segments involved in the local rearrangement directly from experimental data. Results for two different polymers as a function of temperature are presented. © *2005 American Institute of Physics*. [DOI: 10.1063/1.1861881]

I. INTRODUCTION

In the last decade the study of single fluorophores immobilized in polymeric thin films has received increasing research attention. Initially the polymeric matrix helped increase photostability and quantum efficiency of the fluorophores for single molecule studies.[1–4] More and more the situation has reversed and the polymer has become the object of study by single molecule methods.[5–7] Polymer mobility has been probed in the supercooled liquid regime by use of mobility observables[5] and in the glassy state by use of spectroscopic observables.[7–12] At cryogenic temperatures, it has been shown[13] that most of the spectral trails of single molecules show a behavior consistent with the double well potential model of glasses, representing motion of a small group of glass atoms within double well features of the potential energy hypersurface.[14–16] Recently we have shown that lifetime fluctuations of single molecules embedded in a polymer matrix reflect the local segmental mobility of the polymer chains.[7] Free volume theories,[17–20] generally applied to describe molecular properties and physical behavior of polymers, can now be confronted with nanoscopic experiments.

Figure 1 shows the investigated system: a probe molecule is inserted in a poly(styrene) matrix to report on the dynamic competition between segments and voids that surround it. The probe molecule is a highly conjugated molecule adequately described by a simple two-level system, with the ground state $|g\rangle$ and one single singlet excited state $|e\rangle$ of importance. Indeed, the electronic properties of such a molecule are dominated by the presence of delocalized π electrons. The highest occupied molecular orbital (HOMO) is a π orbital, since the electrons in the σ bonds are tightly bound, and the lowest unoccupied molecular orbital (LUMO) is an excited configuration of the π orbitals ($\pi*$). The lowest optical excitation thus corresponds to the promotion of a π electron from the HOMO to the LUMO and vice versa for the emission. The fluorescence lifetime, i.e., the natural decay time between the photon excitation and subsequent Stokes-shifted photon emission is an inherent property of the isolated fluorophore. However, when embedded in a polymer matrix, several processes can alter the lifetime. The fluorescence signal may be quenched due to the appearance of an extra decay channel, such as the intramolecular or intermolecular dissipation of vibrational energy. Due to the interaction of the molecule with its environment, the conformation of the fluorophore may change and still remain optically active.[11] Finally, modifications in the dielectric properties of the fluorophore near surrounding may dramatically affect its fluorescence lifetime.[21] In this paper, we present in detail a theoretical modeling that allowed us to link the experimental observation of asymmetrically varying lifetime

[a)]Electronic mail: renaud.vallee@chem.kuleuven.ac.be
[b)]Electronic mail: n.f.vanhulst@tn.utwente.nl

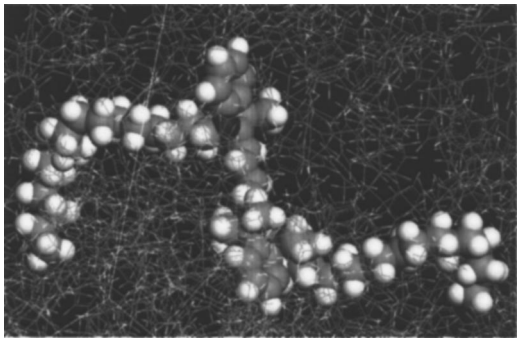

FIG. 1. Two-dimensional representation of a poly(styrene) matrix (lines) embedding a DiD fluorophore (CPK) that reports on its nanolocal environment.

time traces of single molecules to segmental rearrangements of the polymer chains surrounding the fluorophores under study. The connection is mainly based on the merging of an effective-medium dielectric theory[22,23] and a hole theory, such as the Simha–Somcynsky free-volume theory.[19,20]

II. EXPERIMENT

Dye-doped polymer films (70 nm, respectively, 70 and 200 nm) were prepared by spin-coating a solution of 1, 1′-dioctadecyl-3,3,3′,3′-tetramethylindodicarbocyanine (DiD, 5×10^{-10} M, Molecular Probes) and poly(styrene) [PS, 89 300 g/mol, polydispersity index (PI) of 1.06, Polymer Standard Service], respectively, poly(isobutyl methacrylate) (PIBMA, 67 200 g/mol, PI=2.8, custom made by radical polymerization), in toluene onto a cleaned glass substrate. Further annealing was performed in order to remove residual solvent and to relax the stresses induced by the deposition procedure. Annealed films were investigated by atomic force microscopy (Nanoscope III, Digital Instruments, Santa Barbara) to accurately determine the film roughness and thickness, using the so-called "scratch method."[24,25] The choice of the dye was dictated by the facts that it possesses a high fluorescence quantum yield (close to unity), a high absorption cross section of 7.4×10^{-16} cm^2/molecule, and is highly photostable when embedded in a polymer matrix.[1] The absorption and emission spectra of the dyes have maxima at 644 and 665 nm, respectively.[26] PS (T_g=373 K) and PIBMA (T_g=329 K) were chosen because of their different glass transition temperature T_g. This allowed us to probe the polymer properties as a function of temperature, obtaining different deviations from T_g for the two polymers while working at the same absolute temperatures in the laboratory. Molecules were excited with 57 ps pulses at a wavelength of 645 nm and at a repetition rate of 80 MHz, generated by a pulsed diode laser (PicoQuant, PDL 800-B, 100 μW). Bandpass excitation filter (630AF50) was inserted at the entrance of a confocal scanning microscope (CFM, Zeiss inverted microscope) before focusing the circularly polarized light on the sample. The light beam was focused on the sample using an air objective lens (Olympus NA 0.75, 40X). The fluorescence light emitted by the embedded dye was collected through the same objective, separated from the excitation light by use of a dichroic mirror (650DRLP) and a long pass filter (695AF55), polarization selected with a polarization cube, and directed to the small detection areas (160 μm) of two avalanche photodetectors (APDs) (SPCM-AQ-14, EG & G Electro Optics). These APDs determine the arrival time of a photon with an accuracy of 300 ps. Finally, a SPC 500 time-correlated single-photon counting card (TCSPC, Becker & Hickl) was used to record the start-stop events of light excitation and emission by the fluorophore, which allowed us to subsequently determine its fluorescence lifetime. With a pulse repetition rate of 80 MHz, the time window available to record the emitted photons is 12.5 ns. The decay profile was built by sampling all photons in 256 channels, thus resulting in a timing resolution of 50 ps. The accuracy is actually limited by the APDs. The whole setup was computer controlled by custom made LabView software. To localize the molecules, fluorescence intensity images were acquired by scanning the sample over areas of 10×10 μm^2 at a pixel frequency of 2 kHz with a step size of 39 nm/pixel. Time traces of the fluorescence intensity and lifetime were obtained in consecutive experiments on specific molecules that were centered in the laser focus. The experimental determination of fluorescence lifetimes was performed by adding signals of the two TCSPC channels and using a Levenberg–Marquadt method to fit the monoexponential decay profiles obtained by sampling photon arrival times during 200 ms. The background fluorescence was taken into account in the fitting procedure as a constant offset of the fluorescence signal. The procedure was repeated 125 times (or limited by the photobleaching of the fluorophore) to get a full fluorescence lifetime time trace.

III. RESULTS AND DISCUSSION

Figure 2(a) shows the intensity and fluorescence lifetime time trace of a DiD molecule embedded in a 70 nm thick film of PIBMA. While the intensity emitted by the molecule shows only a slight decrease in time, the lifetime exhibits frequent excursions to higher values. The panels in Fig. 2(b), a correlation plot (top) and the fluorescence lifetime distribution (bottom), exemplify the asymmetric behavior of the lifetime with a skewed lifetime distribution and a cloudy correlation plot, elongated towards higher fluorescence lifetime values. This observation essentially raises two questions: Which of the processes that can alter the fluorescence lifetime is responsible for the observed fluctuations? Why is there an asymmetry in the fluctuations?

A. Role of quenching effects

To address our question we first consider the effect of quenching phenomena that can occur in the matrix. The experimentally obtained fluorescence lifetime corresponds to the total lifetime τ_{tot} of the excited single molecule. This contains contributions of both radiative τ_{rad} and nonradiative τ_{nrd} lifetimes:

$$\frac{1}{\tau_{\mathrm{tot}}}=\frac{1}{\tau_{\mathrm{rad}}}+\frac{1}{\tau_{\mathrm{nrd}}}. \tag{1}$$

Clearly, the appearance of extra, fast, nonradiative decay channels in the matrix will contribute to the right-hand side

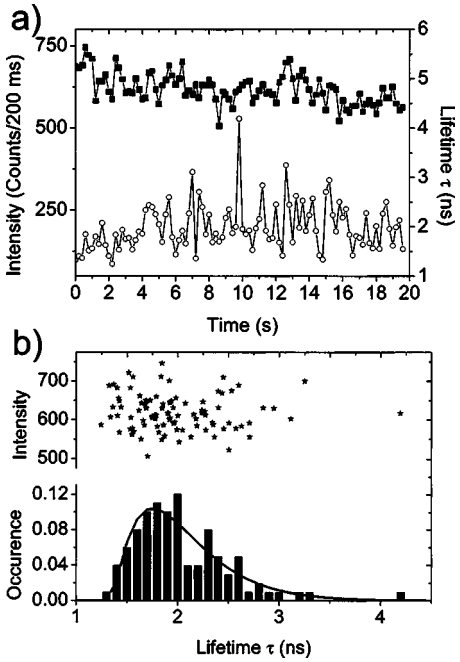

FIG. 2. (a) Fluorescence intensity (squares) and corresponding lifetime (circles) transients of an individual DiD molecule in a 70 nm thick film of PIBMA at an excitation power of 1.2 kW/cm^2. Data were binned in 200 ms time interval. The lifetime makes peculiar excursions towards higher values. (b) Correlation plot (top) and fluorescence lifetime distribution (bottom) of the molecule: Asymmetrical fluctuations of the lifetime results in an elongated, cloudy correlation plot and an asymmetric distribution. The lifetime distribution is fitted with a γ distribution.

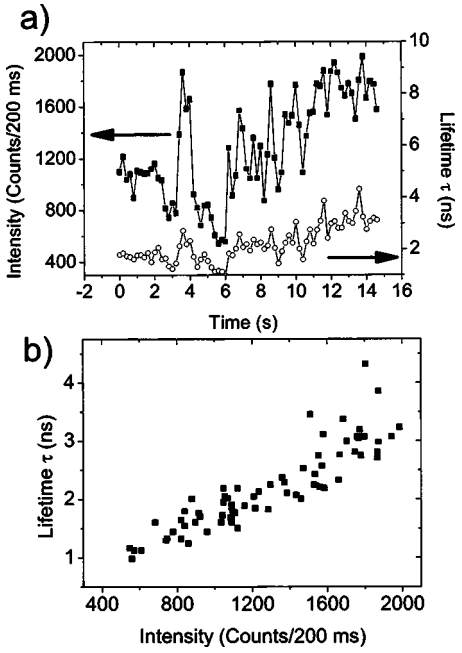

FIG. 3. (a) Fluorescence intensity (squares) and corresponding lifetime (circles) transients of an individual DiD molecule in a 70 nm thick film of PIBMA at an excitation power of 1.2 kW/cm^2. Data were binned in 100 ms time interval. (b) Correlation plot of the molecule. Intensity and lifetime are perfectly correlated, suggesting the aperture of extra-decay channels in the matrix. This correlated behavior has been observed for only two molecules within the 778 investigated molecules.

of this equation, which, in turn, will induce a decrease of the total lifetime. Figure 2(a) shows clearly that variations in the lifetime are towards higher values. In case a quenching phenomenon occurs at a given time, a decrease of the measured lifetime is expected at this time. Only if the single molecule is always subject to the quenching phenomenon, but not at the times of the peaks, can the lifetime time trace of Fig. 2(a) be explained. In that case, however, the mean fluorescence lifetime value of the single molecule should have been lower than the observed 1.8 ns, which is characteristic for this single molecule.[27] Furthermore, simultaneously with the lifetime change, the presence of an extra decay channel will reduce the measured intensity as the quantum efficiency of fluorescence (QE) is given by

$$\mathrm{QE} = \frac{\tau_{\mathrm{tot}}}{\tau_{\mathrm{rad}}}. \tag{2}$$

The fluorophores under study have quantum efficiencies QE close to 1 so that τ_{tot} becomes equal to τ_{rad}, leaving no chance for the aperture of nonradiative decay channels to occur. Of the 778 molecules investigated on the single molecule level, only 2 showed indeed a clear correlation between intensity and fluorescence lifetime, as shown on Fig. 3. For the remaining 776 molecules, this behavior was not observed [Fig. 2(b)].

B. Effect of the molecular conformation

In the electric dipole approximation, the coupling between the molecule and the electromagnetic field is described by the interaction term: $H_{\mathrm{int}} = -\vec{\mu}\cdot\vec{E}$, where $\vec{\mu}$ denotes the dipole moment operator of the molecule and $\vec{E}$ is the electric field operator. In order to obtain the spontaneous emission rate Γ of the molecule, we apply Fermi's golden rule:

$$\Gamma = \frac{2\pi}{\hbar}|\langle e|H_{\mathrm{int}}|g\rangle|^2\rho(\omega), \tag{3}$$

where $\rho(\omega)$ denotes the radiative density of states (RDOS) at the transition frequency ω. In vacuum, the radiative decay rate of the dipole writes[28]

$$\Gamma_0 = \frac{\omega_0^3|\vec{\mu}|^2}{3\pi\epsilon_0\hbar c^3} = \frac{1}{\tau_0}, \tag{4}$$

where τ_0, ω_0, $|\vec{\mu}|$, and ϵ_0 designate the radiative lifetime, the transition frequency, the transition dipole moment of the excited state of the fluorophore for the transition $|e\rangle \rightarrow |g\rangle$, and the dielectric constant of the vacuum, respectively. This equation reveals that a change in the transition frequency or in the transition dipole moment of the fluorophore due to a change of conformation induced by interaction with the environment[11] can be responsible for the observed fluctuations of the lifetime. Through quantum chemistry calculations, we showed[27] that the ground and excited states of the chosen carbocyanine molecule have essentially the same nuclear structure and an electronic density mostly localized on odd- or even-numbered carbon atoms of the polyenic chain (the numbering starting from one of the two nitrogen atoms), respectively. The molecule thus has little vibronic coupling, as is seen by the small Stokes shift of the fluores-

cence emission. Also, the transition dipole moment calculated on the base of these orbital shapes has vanishingly small contributions arising from the polyenic segment; the atomic transition densities are mainly localized on the nitrogen atoms. In order to probe the impact of possible structural changes, due to direct interaction of the fluorophore with the surrounding polymer chains, on the transition dipole moment or on the transition energy of the molecule, we determined the low-cost energy motions of the molecule compatible with thermal agitation at room temperature. The tilting of an aromatic ring with respect to the rest structure fulfilled the requirement. Consequently, we imposed in the structure a gradual tilt of one aromatic ring around the polyenic segment and performed an energy minimization to determine the transition frequency in each case. A change of at most 10% in the fluorescence lifetime was calculated, which cannot explain the large lifetime fluctuations experimentally obtained. Moreover the calculated lifetimes can have both smaller and larger values, while the observed fluctuations are predominantly upwards.

C. Effect of the dielectric medium on the RDOS

In this study, the fluorophore is placed in a polymeric matrix film kept in the frozen glassy state. The embedded fluorophore is immobile, as verified by probing the polarization state of the emitted fluorescence with two orthogonal detection channels. The fluorescent radiation depends on the dielectric properties of the matrix, the size (thickness) of the film, and the reflectivity of the film boundaries. In particular, close to the air-polymer interface, the fluorescence lifetime of a single molecule is known to depend strongly on the orientation of the transition dipole with respect to the interface.[1,26] The fluorescence lifetime is expected to be large as the single molecule emission dipole is oriented perpendicular to the interface.[26] However, the films used in this study are rather thick (around 70–200 nm) so that interfacial effects are negligible. A reorientation of the dye with respect to the air-polymer interface can thus not be responsible for the sporadic elongation of lifetimes observed in a single molecule timetrace [Fig. 2(a)].

The spontaneous rate $\Gamma(\epsilon)$ of the fluorophore inside a homogeneous medium with a dielectric constant ϵ (=2.5 in polystyrene at the emission frequency of the fluorophore) is predicted to follow the $\sqrt{\epsilon}$ dependence of the RDOS:

$$\Gamma(\epsilon) = \sqrt{\epsilon}\Gamma_0. \tag{5}$$

However, this equation pertains to a quantized macroscopic electromagnetic field,[29] while the dipole couples to the local field at the position of the molecule. The microscopic local field differs from the macroscopic field by a correction factor, as described in different models, e.g., empty-cavity, full-cavity, or no-cavity model.[30,31] For substitutional or interstitial fluorophores, it has been shown that, respectively, the empty-cavity and Lorentz-local field factor apply.[32] Here, we apply the empty-cavity factor $L_{\mathrm{emp}}=3\epsilon/(2\epsilon+1)$, since the presence of the fluorophore in the polymer matrix represents an excluded volume for the dipoles constituting the dielectric. Including this factor in the description of the spontaneous emission rate $\Gamma(\epsilon)$, one obtains the modified expression[28]

$$\Gamma(\epsilon) = \sqrt{\epsilon}L_{\mathrm{emp}}^2\Gamma_0 = \frac{9\epsilon^{5/2}}{(2\epsilon+1)^2}\Gamma_0 = \frac{1}{\tau}, \tag{6}$$

where τ is the fluorescence lifetime of the DiD molecule in the polymer matrix.

So far, we have considered the polymer matrix as a homogeneous medium of dielectric constant ϵ. However, polymer chain segments move in time in the matrix at room temperature so that the mass density of the probe molecule environment is continuously and locally modified. We describe the system as an effective medium consisting of polymer segments and voids competing to occupy the cells of a cubic lattice. This motion results in corresponding changes of the polarizabilities of the cells surrounding the probe molecule placed at the center of the lattice. Local mass density changes are thus directly related to changes of the local radiative density of states of the probe, which in turn modify the local dielectric constant of its near surrounding. This local effective dielectric constant ϵ (Ref. 22) is defined in such a way as to incorporate the effect of the moving holes in the polymer matrix surrounding the probe molecule:

$$\epsilon = h\epsilon_{\mathrm{vac}} + (1-h)\epsilon_{\mathrm{pol}}, \tag{7}$$

where h is the fraction of holes present in the medium, $\epsilon_{\mathrm{vac}}=1$ and $\epsilon_{\mathrm{pol}}=2.5$ designate the vacuum and polymer (PS) dielectric constant, respectively. This equation clearly shows that a temporal fluctuation of the fraction of holes present around the fluorophore will cause a variation of the local effective dielectric constant, which in turn will induce a change in the lifetime of the fluorophore [Eq. (6)].

D. Cell and hole theories

Having established a connection between lifetime fluctuations and polymer density fluctuations, we will address the nature of the fluctuations in molecular packing. To this end the use of cell models is highly appropriate. Indeed, such molecular models are based on the development of a proper partition function, from which an equation of state (EOS) is determined.[33] This EOS is intimately connected with the macroscopic pressure-volume-temperature, *p-V-T*, properties of the bulk polymer. A cell model thus allows one to relate macroscopic to local, molecular properties of the polymer. The Lennard-Jones and Devonshire cell model for liquids constitutes a prototype cell model.[34,35] In this model, the particles are localized in singly occupied spherical cells of volume $v=V/N$ on the sites of a fully occupied lattice. The particles are assumed to move independently within the cell and can interact with z nearest neighbors smeared around the surface of a larger concentric sphere. The Helmholtz free energy of the system is then given by

$$F = -Nk_BT\ln(v_f\sigma_c) + \frac{NE_0}{2}, \tag{8}$$

where k_B is Boltzmann's constant, v_f is the free volume per cell, σ_c is the communal entropy term, which accounts for the entropy lost due to the localization of the particles within cells, and E_0 is the ground state energy per particle. The cell

potential, defined as the interaction energy between the particle within the cell and neighboring particles, is calculated by use of the 12-6 Lennard-Jones potential. By its integration over the volume of the cell, the cell potential permits the determination of the free volume per cell, hence the Helmholtz free energy, and finally the equation of state.

For polymer chains, the Lennard-Jones and Devonshire cell model for liquids was applied to the polymer fluid already by Prigogine, Bellemans, and Mathot.[36] Two distinct sets of modes are in this case assumed to contribute to the partition function: the internal modes associated with internal motions and the external modes associated with intermolecular interactions. Only the external modes affect the *p-V-T* properties of the system. The polymer chains are divided into segments having $3f$ external degrees of freedom, with f ($f<1$) a constant that accounts for the intermolecular constraints on the segments. The Prigogine EOS is obtained by using the square-well approximation to the 6-12 Lennard-Jones potential, with hexagonal close packing for the cell geometry. In this Prigogine model, only changes of the cell volume contribute to the thermal expansion of the system and do not give enough entropy to describe the liquid state.

To avoid this drawback of cell models, hole theories were developed. Changes in cell volume are still allowed, but vacant cells or holes are introduced in the lattice to describe the extra entropy change in the system as a function of volume and temperature. The Simha–Somcynsky (SS) model[19,20] considers a system of N s-mer molecules, occupying a fraction y of the total number of available sites. The model uses the square-well approximation of the 6-12 cell potential and completes the Prigogine model with the introduction of a mixing term $g(N,y)$, which increases the entropy of the system (mixing of molecules and empty sites à la Flory–Huggins,[37] assuming that all holes have the same size). The Helmholtz free energy of the system is written as

$$F = -cNk_BT\ln[v_f(V,y)] + \frac{E_0(V,y)}{2} - k_BT\ln[g(N,y)], \tag{9}$$

where v_f is the free volume per segment, having 3 of the total number $3c$ of external degrees of freedom attributed to a chain. $g(N,y)=y^{-N}(1-y)^{-Ns(1-y)/y}$ is the combinatory factor given by the Flory–Huggins theory. Given the cell volume $\omega=yV/Ns$, the potential energy of the system with all segments placed in their rest positions is

$$E_0 = yNqz\epsilon^*\left[1.011\left(\frac{v^*}{\omega}\right)^4 - 2.409\left(\frac{v^*}{\omega}\right)^2\right], \tag{10}$$

where ϵ^* and v^* are the characteristic energy (potential minimum) and volume (repulsive or hard-core volume) per segment, respectively. $qz=s(z-2)+2$ is the number of nearest neighbors sites per chain. The prefactors of the attractive and repulsive parts of the Lennard-Jones 6-12 potential account for effects of higher coordination shells on the internal energy. In order to obtain the free energy as a function of volume and temperature, the determination of the occupancy fraction $y(V,T)$ is needed. This is achieved by minimization of the Helmholtz free energy with respect to this variable:

TABLE I. Characteristic pressure p^*, volume V^*, temperature T^*, and expansion coefficient γ for the polymers.

Polymer	p^* (bar)	V^* (cm/g)	T^* (K)	γ ($p=1$ bar)
PS	7453	0.9598	12 680	2.24×10^{-4}
PIBMA	5010	0.9320	10 070	6.58×10^{-4}

$$\left(\frac{\partial F}{\partial y}\right)_{V,T} = 0. \tag{11}$$

The relation

$$p = \left(-\frac{\partial F}{\partial V}\right)_{\omega,T} \tag{12}$$

then allows one to calculate the reduced EOS from the free energy F of the system:

$$\frac{\tilde{p}\tilde{V}}{\tilde{T}} = \frac{(y\tilde{V})^{1/3}}{(y\tilde{V})^{1/3} - 2^{-1/6}y} - \frac{2y}{\tilde{T}}\left(\frac{1.2045}{(y\tilde{V})^2} - \frac{1.011}{(y\tilde{V})^4}\right), \tag{13}$$

with $\tilde{V}=V/(Nsv^*)$, $\tilde{T}=ck_BT/(qz\epsilon^*)$, and $\tilde{p}=psv^*/(qz\epsilon^*)$ being the reduced variables of state. The scaling factors are the SS model characteristic pressure p^*, volume V^*, and temperature T^* of the considered polymer.

It is interesting to note here that knowledge of both the SS model characteristic parameters and the actual experimental *p-V-T* conditions allows one to determine the occupancy fraction y and hence the fractional mean free volume $h_{av}=1-y$ present in the system by use of the simple SS equation of state. The volume V occupied by the system is determined for a given temperature T and pressure p ($p=1$ bar in our experiment) as

$$V = V_g + \gamma(T - T_g), \tag{14}$$

where T_g, V_g, and γ are the glass transition temperature, the occupied volume at T_g, and the expansion coefficient of the considered polymer.

Table I summarizes the information needed to perform such calculations for both PS and PIBMA. These parameter values are easily found in the specialized literature in the case of PS.[38,39] We fitted the P,V,T data given in the book of Zoller[40] to the Simha–Somcynsky equation of state to find the appropriate values in the case of PIBMA.

Due to thermal fluctuations, the free volume is not constant in time at every position. From one locally defined region on the lattice (a local segmental rearrangement cell) to another region,[41,42] the chain segments can rearrange very differently. A mean-squared deviation from the mean free volume can be calculated owing to the relation:

$$\langle \delta h^2 \rangle = kT \Big/ \left(\frac{\partial^2 F}{\partial y^2}\right). \tag{15}$$

By assuming the number of segments s per chain to be big enough (high molecular weight polymer) and the flexibility ratio $s/3c=1$, which corresponds to an ideally flexible s-mer without soft side chain motions, the deviation of the mean free volume around the average h_{av} is

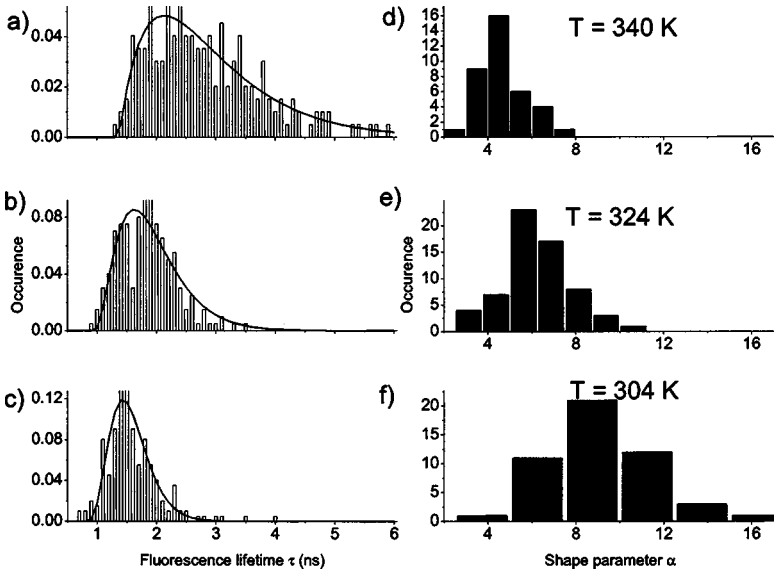

FIG. 4. (a)–(c) Fluorescence lifetime distributions of three individual DiD molecules embedded in a 200 nm thick film of PIBMA. Each lifetime distribution fitted is with a γ distribution. As the lifetime distribution gets more symmetric, the shape parameter of the γ distribution α increases [from (a) to (c)]. (d)–(f) Distributions of the shape parameters α for DiD molecules embedded in the same film at three different temperatures. Shape parameter values decrease with temperature: the asymmetry of the lifetime distributions becomes more and more pronounced as the temperature increases.

$$\langle \delta h^2 \rangle = \frac{1}{N_s} f(y, \tilde{V}, \tilde{T}), \tag{16}$$

with

$$f(y,\tilde{V},\tilde{T}) = \left\{ \frac{1}{y^2}\left[1 + \frac{2}{y}\ln(1-y) + \frac{1}{1-y}\right] + \frac{1}{3}\frac{(\sqrt{2}y\tilde{V})^{2/3} - 8/3y(\sqrt{2}y\tilde{V})^{1/3} + 3y^2}{y^2[(\sqrt{2}y\tilde{V})^{1/3} - y]^2} + \frac{1}{3y\tilde{T}}[6.066(y\tilde{V})^{-4} - 2.409(y\tilde{V})^{-2}] \right\}^{-1}. \tag{17}$$

The assignment of the flexibility ratio to unity serves to define the segment. It corresponds, with this assignment, to 1 monomer of the *s*-mer, which replaces the real chain consisting of *n* repeat units. In a real structure, the segment encompasses more repeat units. In poly(*n*-butyl methacrylate), for example, the segmental molar mass turns out to be one-half of the average molar mass per back bone unit.[43] The volume of the segment is in fact a compromise between size and fine structure of the repeat unit. In Eq. (16), $N_s = N.s$ is the number of monomers in the region containing all segments involved in a local segmental rearrangement.

Taking the mean free volume $\langle h_{\mathrm{av}} \rangle$ and the deviation from the mean free volume $\langle \delta h^2 \rangle$ as the first two moments, a γ distribution $g(x)$ of free volume has been used by several authors.[44,41] The distribution $g(x)$ of a lower bounded continuous variable x is fully characterized by its shape (α) and scale (β) parameters:[45]

$$g(x) = \frac{\beta(\beta x)^{\alpha-1} e^{-\beta x}}{\Gamma(\alpha)}, \tag{18}$$

where $\Gamma(\alpha)$ stands for the gamma function. The first two moments of the distribution are given by $x_{\mathrm{av}} = \alpha/\beta$, $\langle \delta x^2 \rangle_{\mathrm{av}} = \alpha/\beta^2$. Equations (16) and (17) clearly show that the use of such a distribution to relate the macroscopic and molecular properties of the system implies the knowledge of the number of segments N_s involved in a local segmental rearrangement cell. But, as this parameter is local and not directly accessible by usual bulk experiments, its value has been fixed more or less arbitrarily in earlier work.[44,41] For poly(styrene), for example, a $N_s = 40$ value has been arbitrarily chosen.

E. Fluctuating surrounding–effective medium theory

We have investigated and quantified the fluorescence lifetime behavior of 778 individual probe molecules embedded in different polymer matrixes (PS and PIBMA) at various temperatures. For each single molecule trajectory [Fig. 2(a)] lasting at least 15 s we were able to build up a reliable distribution of fluorescence lifetimes. The experimental lifetime distributions were found to be best fitted with a γ distribution [Fig. 2(b)]. From the fitted γ distribution for each molecule [Figs. 4(a)–4(c)], we extracted a characteristic shape parameter α. A γ distribution is a positively skewed distribution. The more skewed is the distribution, the lower is the shape parameter α. At each given temperature, collecting the shape parameters of 30 to 60 of these molecules, we constructed the distribution of the shape parameter. Figures 4(d)–4(f) show the shape distributions for three different temperatures in the case of DiD embedded in a 200 nm thick film of PIBMA: upon increasing the temperature, the average shape value α as well as the width of the shape parameter distribution were found to decrease.

The lowering of the shape parameter corresponds to an increased upwards departure of the fluorescence lifetime with respect to its mean value. In view of Eqs. (6) and (7), this upwards departure of the lifetime is due to a local increase of the hole fraction in the immediate vicinity of the fluorophore. Consequently, the observation of a decreasing function of the shape parameter α with temperature indicates a corresponding increasing function of the amount of holes surrounding the fluorophore as the temperature is increased. This temperature dependence corroborates the fact that density fluctuations in the polymer are the main actor in the observed lifetime fluctuations.

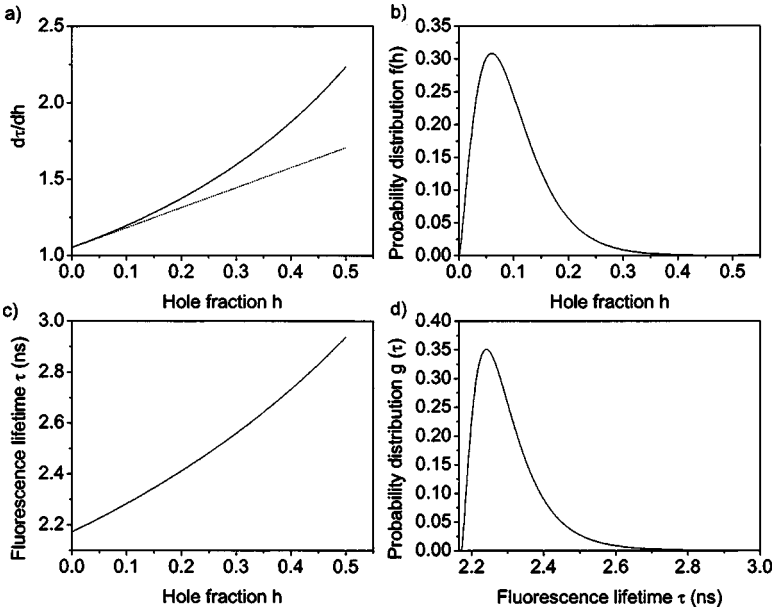

FIG. 5. (a) Ratio of the fluorescence lifetime and hole fraction distributions as a function of the hole fraction h present in the system. For small hole fractions, the dependence is smoothly linear, which means that both distributions have the same shape. (b) Simulated γ distribution of hole fraction, characterized by a mean value of 10% and a mean-squared standard deviation of 0.4%. The shape parameter α of the distribution is 2.5. (c) Dependence of the fluorescence lifetime of the dye embedded in the matrix on the fraction of holes present in the system. (d) Corresponding distribution of the fluorescence lifetime. τ_{vac} has been set equal to 5 ns to perform the calculation. The shape of this distribution is similar to the one in (b): 2.307.

Following standard statistical theory,[46] performing a substitution of the variable τ (fluorescence lifetime) into h (hole fraction) [Eqs. (6) and (7)] lead to a change of the probability density $f(\tau)$ into

$$g(h) = f(\tau)\left|\frac{d\tau}{dh}\right| \tag{19}$$

and vice versa. The following expression relates the two probability densities:

$$\frac{d\tau}{dh} = -\frac{\tau_{vac}}{18}(2h\epsilon_{vac} + 2\epsilon_{pol} - 2\epsilon_{pol}h + 1) \times(\epsilon_{vac} - \epsilon_{pol})\frac{2h\epsilon_{vac} + 2\epsilon_{pol} - 2\epsilon_{pol}h + 5}{(h\epsilon_{vac} + \epsilon_{pol} - \epsilon_{pol}h)^{7/2}}. \tag{20}$$

In a first order development for small h values (generally $h \leqslant 10\%$), this ratio is

$$\frac{d\tau}{dh} = ah + b, \tag{21}$$

where a and b are given by

$$a = \frac{\tau_{vac}(\epsilon_{vac} - \epsilon_{pol})^2(6\epsilon_{pol}^2 + 30\epsilon_{pol} + \frac{35}{2})}{18\epsilon_{pol}^{9/2}}, \tag{22}$$

$$b = -\frac{\tau_{vac}(\epsilon_{vac} - \epsilon_{pol})^2(4\epsilon_{pol}^2 + 12\epsilon_{pol} + 5)}{18\epsilon_{pol}^{7/2}}. \tag{23}$$

The relative error introduced by neglecting higher order terms in the exact analytical treatment is about 1% (1.1% for the hole fraction $h=10\%$) [Fig. 5(a)]. In the effective medium considered here, values of a and b are equal to 1.308 and 1.052, respectively. This smooth linear relationship means that the fluorescence lifetime and hole fraction probability densities have the same form, i.e., can both be described by γ distribution. Indeed, Fig. 5(b) shows an arbitrary chosen γ distribution of the fraction of holes present in the medium, characterized by its first two moments $h_{av} = 10\%$ and $\langle \delta x^2 \rangle_{av} = 0.4\%$. Its shape α is equal to 2.5. Figure 5(c) shows the relationship between the fluorescence lifetime τ and the fraction of holes h in this case. Figure 5(d) shows the corresponding distribution of fluorescence lifetimes. It is found to be also a γ distribution with the same shape as in Fig. 5(b) and with a relative error of only 3.6%. This relative error constitutes a maximum, as 10% of holes in average in the system is considered to be an upper limit in polymer theories.

F. Effective medium and hole theories

In the effective medium approach, by assuming that an effective dielectric constant ϵ represents adequately the dielectric properties of the local surrounding of the probe molecule, we showed that γ distributed fluorescence lifetimes result in γ distributions of the fraction of holes surrounding the dye molecule, with an identical shape parameter. Furthermore, the number of segments involved in a local segmental rearrangement cell is a linear function of the shape parameter α of the hole fraction γ distribution:

$$N_s = \alpha f(h, \tilde{V}, \tilde{T}). \tag{24}$$

As a consequence, for given experimental p-V-T conditions, we propose to relate directly the number of segments involved in a local segmental rearrangement cell with the shape parameters of the lifetime distributions as obtained in the single molecule experiments. The shape distributions (Fig. 4) can therefore be converted into corresponding distributions of the number of segments N_s involved in a local segmental rearrangement cell. Figure 6 shows the peak positions of N_s distributions as a function of temperature for PIBMA and PS films. The striking feature of this plot is the appearance of a common behavior: the number of segments involved in a segmental rearrangement cell is a decreasing function of temperature for both polymers. Linear fits and extrapolations of the experimental curves indicate that typically six segments are involved in a rearrangement cell at the glass transition temperature in the case of PIBMA while four segments only are involved in the case of PS. As previously

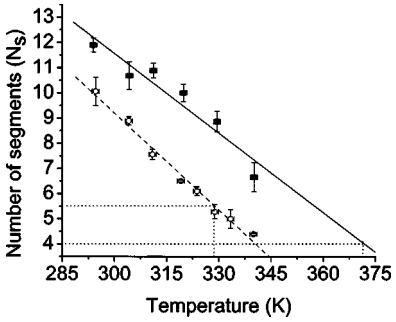

FIG. 6. Number of segments N_s involved in a segmental rearrangement cell as a function of temperature for a PS (close squares, T_g=373 K, 70 nm thick film) and for a PIBMA (open circles, T_g=329 K, 200 nm thick film) matrix. In both cases, the number of segments decreases with temperature. Linear fits and extrapolation of the two curves are also represented on this graph (straight line for PS and dashed line for PIBMA).

mentioned, the volume of a segment is a compromise between size and fine structure of a repeat unit of the chosen polymer. It is thus not surprising to see the number of segments implied in a rearrangement cell at T_g being different for PS and PIBMA (Fig. 6).

At this point of the discussion, it is tempting to make a link between the rearrangement cells just discussed and the vault picture described recently in the literature. Following Donth and co-workers,[47] a vault is a frozen cooperativity shell surrounding a Glarum defect. This defect is still working in a reduced temperature interval below T_g. The difference in thermal contraction between the frozen shell and the mobile defect generates additional free volume with respect to a situation without vault. Below a minimal number $N_\alpha^{\min}(T_g)$ of monomeric units in the cooperativity shell, no vaults can be formed. Using a von Laue approach instead of a Gibbs distribution analysis of the glass transition, Donth and co-workers determined $N_\alpha(T_g)=15$ and $N_\alpha(T_g)=12$ in the case of poly (propyl methacrylate)(PPMA), poly (*n*-butyl methacrylate)(PnBMA), respectively. The order of this minimal number is consistent with the formation of a first coordination cell of structure in the glassy polymer. In this picture, the number of monomeric units in the cooperativity shell is a decreasing function of temperature $N_\alpha(T<T_g) > N_\alpha^{\min}(T_g)$, which is consistent with the results of Fig. 6. Also, the "mean" number $N_s=6$ of segments involved in a rearrangement cell at T_g in the case of PIBMA is of the same order of magnitude as $N_\alpha^{\min}(T_g)$ determined in the cases of PPMA and PnBMA.

IV. CONCLUSIONS

In this paper, we have demonstrated that single molecule spectroscopy is able to give quantitative information about the polymer segmental dynamics. Specifically, fluorescence lifetime fluctuations of the probe molecule have been shown to result from local density fluctuations of its immediate surrounding. Using the Simha–Somcynsky theory, we determined the number of segments involved in a local segmental rearrangement cell as a function of temperature. Typically, four to six segments are found to be involved in a rearrangement cell around T_g. All steps involved in the derivation connecting the observation of single molecule fluorescence lifetime fluctuations to segmental motions of polymer chains around the investigated molecules have been explained. The observed common decrease of the number of segments involved in a local segmental rearrangement cell as the temperature is increased for two different polymers illustrates the power of the approach.

Very recently,[48] we have developed a microscopic model to describe the observed temporal fluctuations of the fluorescence lifetime of single molecules embedded in a polymer at room temperature. The model represents the fluorescent probe and the polymer matrix on the sites of a cubic lattice, and introduces voids in the matrix to account for its mobility. We have generalized Lorentz's approach to dielectrics by considering three domains of electrostatic interaction of the probe molecule with its nanoenvironment: (i) the probe molecule with its elongated shape and its specific polarizability, (ii) the first few solvent shells with their discrete structure and their inhomogeneity (monomers with their specific polarizability and voids as sites of zero polarizability), and (iii) the remainder of the solvent at larger distances, treated as a continuous dielectric. The model is validated by comparing its outcome for homogeneous systems with those of existing theories. When realistic inhomogeneities (voids) are introduced, the model correctly explains the observed fluctuations of the lifetimes of single molecules. By increasing the fraction of voids in the system (by analogy to an increase in temperature), the simulated fluorescence lifetime distributions get more and more asymmetric, in agreement with the results of Fig. 4. The model points to the relevance of local-field effects in single molecule experiments. Atomistic simulations of the system are currently under investigation.

ACKNOWLEDGMENTS

The Council for Chemical Sciences of the Netherlands Organization for Scientific Research (NWO-CW) is gratefully acknowledged for supporting this research (N.T.). R.A.L. acknowledges the FWO (Belgian Funds for Scientific Research) for a postdoctoral fellowship in Leuven.

[1] J. J. Macklin, J. K. Trautman, T. D. Harris, and L. E. Brus, Science **272**, 255 (1996).
[2] X. S. Xie and J. K. Trautman, Annu. Rev. Phys. Chem. **49**, 441 (1998).
[3] D. A. Vanden Bout, W.-T. Yip, D. H. Hu, T. M. Swager, and P. F. Barbara, Science **277**, 1074 (1997).
[4] J. A. Veerman, M. F. García-Parajó, L. Kuipers, and N. F. van Hulst, Phys. Rev. Lett. **83**, 2155 (1999).
[5] L. A. Deschesnes and D. A. Vanden Bout, Science **292**, 255 (2001).
[6] N. B. Bowden, K. A. Willets, W. E. Moerner, and R. M. Waymouth, Macromolecules **35**, 8122 (2002).
[7] R. A. L. Vallée, N. Tomczak, L. Kuipers, G. J. Vancso, and N. F. van Hulst, Phys. Rev. Lett. **91**, 038301 (2003).
[8] A. P. Bartko and R. M. Dickson, J. Phys. Chem. B **103**, 3053 (1999).
[9] R. A. L. Vallée, M. Cotlet, J. Hofkens, F. C. De Schryver, and K. Müllen, Macromolecules **36**, 7752 (2003).
[10] R. A. L. Vallée, N. Tomczak, L. Kuipers, G. J. Vancso, and N. F. van Hulst, Chem. Phys. Lett. **384**, 5 (2003).
[11] R. A. L. Vallée, M. Cotlet, M. Van Der Auweraer, J. Hofkens, K. Müllen, and F. C. De Schryver, J. Am. Chem. Soc. **126**, 2296 (2004).
[12] N. Tomczak, R. A. L. Vallée, E. M. H. P. van Dijk, L. Kuipers, N. F. van Hulst, and G. J. Vancso, J. Am. Chem. Soc. **126**, 4748 (2004).
[13] A.-M. Boiron, Ph. Tamarat, B. Lounis, and M. Orrit, Chem. Phys. **247**, 119 (1999).
[14] E. Geva, P. D. Reilly, and J. L. Skinner, Acc. Chem. Res. **29**, 579 (1996).
[15] E. Geva and J. L. Skinner, J. Phys. Chem. B **101**, 8920 (1997).

[16]E. Geva and J. L. Skinner, J. Chem. Phys. **109**, 4920 (1998).
[17]M. H. Cohen and D. Turnbull, J. Chem. Phys. **31**, 1164 (1959).
[18]D. Turnbull and M. H. Cohen, J. Chem. Phys. **52**, 3038 (1970).
[19]R. Simha and T. Somcynski, Macromolecules **2**, 342 (1969).
[20]R. Simha, Macromolecules **10**, 1025 (1977).
[21]E. Yablonovitch, T. J. Gmitter, and R. Bhat, Phys. Rev. Lett. **61**, 2546 (1988).
[22]D. E. Aspnes, Am. J. Phys. **50**, 704 (1982).
[23]D. J. Bergman, Phys. Rev. Lett. **44**, 1285 (1980).
[24]C. Tonthat, A. G. Shard, and R. H. Bradley, Langmuir **16**, 2281 (2000).
[25]R. F. M. Lobo, M. A. Pereira-da-Silva, M. Raposo, R. M. Faria, and O. N. Oliveira, Jr., Nanotechnology **10**, 389 (1999).
[26]R. A. L. Vallée, N. Tomczak, H. Gersen, E. M. H. P. van Dijk, M. F. García-Parajó, G. J. Vancso, and N. F. van Hulst, Chem. Phys. Lett. **348**, 161 (2001).
[27]R. A. L. Vallée, G. J. Vancso, N. F. van Hulst, J.-P. Calbert, J. Cornil, and J. L. Brédas, Chem. Phys. Lett. **372**, 282 (2003).
[28]R. J. Glauber and M. Lewenstein, Phys. Rev. A **43**, 467 (1991).
[29]G. Nienhuis and C. Th. J. Alkemade, Physica B & C **81**, 181 (1976).
[30]G. M. Kumar, D. N. Rao, and G. S. Agarwal, Phys. Rev. Lett. **91**, 203903 (2003).
[31]F. J. P. Schuurmans, D. T. N. de Lang, G. H. Wegdam, R. Sprik, and A. Lagendijk, Phys. Rev. Lett. **80**, 5077 (1998).
[32]F. J. P. Schuurmans, P. de Vries, and A. Lagendijk, Phys. Lett. A **264**, 472 (2000).
[33]L. D. Landau and E. M. Lifshitz, *Statistical Physics* (Pergamon, New York, 1980).
[34]J. E. Lennard-Jones and A. F. Devonshire, Proc. R. Soc. London, Ser. A **178**, 401 (1941).
[35]J. E. Magee and N. B. Wilding, Mol. Phys. **100**, 1641 (2002).
[36]I. Prigogine, A. Bellemans, and V. Mathot, *The Molecular Theory of Solutions* (North-Holland, Amsterdam, 1957).
[37]G. Strobl, *The Physics of Polymers, Concepts for Understanding Their Structure and Behavior* 2nd ed. (Springer, Berlin, 1997).
[38]A. Quach and R. Simha, J. Appl. Phys. **42**, 4592 (1971).
[39]H. Oels and G. Rehage, Macromolecules **10**, 1036 (1977).
[40]P. Zoller and D. J. Walsh, *Standard Pressure-Volume-Temperature Data for Polymers* (Technomic Publishing, Lancaster, PA, 1995).
[41]R. E. Robertson, in *Computational Modeling of Polymers, Free-Volume Theory and Its Application to Polymer Relaxation in the Glassy State*, edited by J. Bicerano (Marcel Dekker, New York, 1992).
[42]R. E. Robertson, R. Simha, and J. G. Curro, Macromolecules **17**, 911 (1984).
[43]O. Olabisi and R. Simha, Macromolecules **8**, 211 (1975).
[44]J. Liu, Q. Deng, and Y. C. Jean, Macromolecules **2**, 7149 (1993).
[45]J. K. Patel, C. H. Kapadia, and D. B. Owen, *Statistics: Textbooks and Monographs* (Marcel Dekker, New York, 1976), Vol. 20.
[46]M. R. Spiegel, *Probability and Statistics* (McGraw-Hill, New York, 1975).
[47]M. Beiner, S. Kahle, S. Abens, E. Hempel, S. Hing, M. Meissner, and E. Donth, Macromolecules **34**, 5927 (2001).
[48]R. A. L. Vallée, M. Van Der Auweraer, F. C. De Schryver, D. Beljonne, and M. Orrit, ChemPhysChem **6**, 81 (2005).